Production of Charged Pions in Collisions of 450-Mev Protons with Various Nuclei*†

ENDRE LILLETHUN‡
The Enrico Fermi Institute for Nuclear Studies and Physics Department, The University of Chicago, Chicago, Illinois
(Received August 21, 1961)

The differential production cross sections for positive and negative pions by 450-Mev protons on Be, C, Al, Cu, Sn, Sb, Au, Pb, and U have been measured for several pion energies. The energy spectra were measured for carbon at 21.5° and 60° in the laboratory. The variation of cross section as a function of atomic mass number is compared to theoretical curves based on a model where the nucleus is assumed to have a surface layer of neutrons. There is good agreement between the data and the theoretical predictions. The energy spectrum at 21.5° for carbon shows that the positive pions are produced with energies up to the energy expected for the reaction $p+C^{12} \rightarrow \pi^+ + C^{13}$ with the final carbon nucleus left unexcited. The spectrum for negative pions, however, goes to zero at a lower energy, consistent with the fact that a similar two-body reaction is not possible.

I. INTRODUCTION

THE production of charged pions in proton-nucleus collisions has been studied in several experiments.[1–6] The experiments are listed in Table I, showing the energy of the incident protons, the targets employed, and the energy, charge, and emission angle of the observed pions.

The relative differential cross section for photoproduction of 50-Mev charged pions from nuclei over a relatively wide range of A has been shown[7] to follow approximately an $A^{\frac{2}{3}}$ law, as one might expect on the assumption that the pion production takes place on the surface of the nucleus. The experiment by Clark[1] on the production of 40-Mev charged pions by 240-Mev protons on nuclei showed that this simple law was not followed in proton-nucleus production. The cross section as function of atomic mass number (A-spectrum) did not increase as fast as $A^{\frac{2}{3}}$. Since the observation angles for positive and negative pions were different, a direct comparison between the shape of the A-spectra of pions of different charge was not possible.

The experiment by Sagane and Dudziak[2] showed a great difference in the A-spectra of positive and negative pions, produced and observed under identical conditions. The data, obtained for pions of energies between 12.5 and 33 Mev, showed that the π^+ to π^- ratio decreased with increasing mass number for all pion energies, but with a steepness depending on the energy. Most of these variations in the ratio can be explained by the Coulomb interaction of the nucleus with the pion. With a Coulomb barrier, seen by the positive pion, of the order of 10 Mev for heavy nuclei, it is clear that such pions in the energy range considered will undergo a considerable attenuation.

The experiments by Block *et al.*[3] and Merritt *et al.*[4] measured the production cross section mainly for two heavy elements. This, together with rather poor statistical accuracy, make it difficult to draw any conclusion about the A-spectra from these experiments.

Imhof *et al.*[5] made an experimental and theoretical study of the effect of the momentum distribution in the nuclei on the pion production. They studied cases where the struck nucleon needed from 184 to 391 Mev/c in order to produce a pion of the energy under consideration. With an average Fermi momentum of about 220 Mev/c, the sensitivity to varying momentum distributions was quite high. They observed appreciable effects corresponding to increasing Fermi momenta with increasing atomic mass number for the light elements only.

The behavior of the A-spectra of positive pions was explained in general by Gasiorowicz[8] by taking into account the Coulomb interaction and the attenuation of the incoming proton as it penetrates the nucleus, together with the attenuation of the outgoing pion within the nucleus. The production of pions was assumed to occur in proton-nucleon collisions, where the nucleons were assumed to have the same momentum distribution in all elements. He also assumed different distributions for protons and neutrons in the nucleus, with the protons reaching only to 0.9 times the nuclear radius. In the case of positive pions, assuming that the majority of them are produced on protons, this would in effect put an absorptive layer around the effective production volume. The negative pions, being produced on the neutrons, would not see such a layer. As the

* Research supported by a joint program of the Office of Naval Research and the U. S. Atomic Energy Commission.
† A thesis submitted to the Department of Physics, the University of Chicago, in partial fulfillment of the requirements for the Ph.D. degree.
‡ Now at CERN, Geneva, Switzerland.
[1] D. L. Clark, Phys. Rev. **87**, 157 (1952).
[2] R. Sagane and W. F. Dudziak, Phys. Rev. **92**, 212 (1953); University of California Radiation Laboratory Internal Reports UCRL-2304 and 2317, 1953 (unpublished).
[3] M. M. Block, S. Passman, and W. W. Havens, Jr., Phys. Rev. **88**, 1239, 1247 (1952).
[4] J. Merritt and D. A. Hamlin, Phys. Rev. **99**, 1523 (1955). D. A. Hamlin, M. Jakobson, J. Merritt, and A. Schulz, *ibid.* **84**, 857 (1951).
[5] W. Imhof, H. T. Easterday, and V. Perez-Mendez, Phys. Rev. **105**, 1859 (1957).
[6] A. G. Meshkovskii, Iu. S. Pligin, Ia. Ia. Shalamov, and V. A. Shebanov, Soviet Phys.—JETP **4**, 842 (1957) and **5**, 1085 (1957). A. G. Meshkovskii, Ia. Ia. Shalamov, and V. A. Shebanov, *ibid.* **6**, 463 (1958).
[7] R. M. Littauer and D. Walker, Phys. Rev. **83**, 206 (1951).
[8] S. Gasiorowicz, Phys. Rev. **93**, 843 (1954).

TABLE I. A list of experiments performed to study the dependence on atomic mass number of the charged pion production by protons.

Authors	Proton energy (Mev)	Targets	Pion energy (Mev)	Pion charge	Emission angle in the lab (degrees)
Clark[a]	240	Be, C, Al, Cu, Ag, W, Pb	40	+ −	130–150 30– 50
Merritt *et al.*[b]	335	Be, C, Al, Fe, Cu, Ag, Pb Be, B^{10}, B, C C, Cu, Pb	53 34–129 52, 88, 147	+	0
Sagane and Dudziak[c]	340	Be, C, Al, Cu, Ag, Pb	12.5, 27, 33	±	90
Imhof *et al.*[d]	340	Li, Be, B^{10}, B^{11}, C, Al, Cu, Ag, Pb Li, Be, B^{10}, B^{11}, C	36 63	+	135
Block *et al.*[e]	381	H, D, C, Cu, Pb D, C, Cu, Pb	20–120	+ −	90
Present experiment	450	Be, C, Al, Cu, Sn, Sb, Au, Pb, U	83–236 132–200	+ −	21.5 21.5
		C, Cu, Au, Pb, U	149 99	+ −	60 60
Meshkovskii *et al.*[f]	660	Li, Be, C, Al, Cu	70–300 90–300	+ −	45
		Ag, Pb	158 157	+ −	

[a] See reference 1. [b] See reference 4. [c] See reference 2. [d] See reference 5. [e] See reference 3. [f] See reference 6.

neutron layer becomes thicker with increasing atomic number, the effect on the π^+ to π^- ratio would be to decrease it with increasing atomic number. With the available data on positive pion production, Gasiorowicz was not able to decide whether a neutron shell is present or not.

This question came up again in the interpretation of the experiments by Meshkovskii *et al.*[6] in which they measured the production cross section for 157-Mev positive and negative pions by 660-Mev protons on various nuclei. The π^+ to π^- ratio appeared to go through a maximum for carbon, the only nucleus used for which the number of protons equals the number of neutrons. This is consistent with a neutron shell roughly proportional to the number of neutrons exceeding the number of protons in a nucleus.

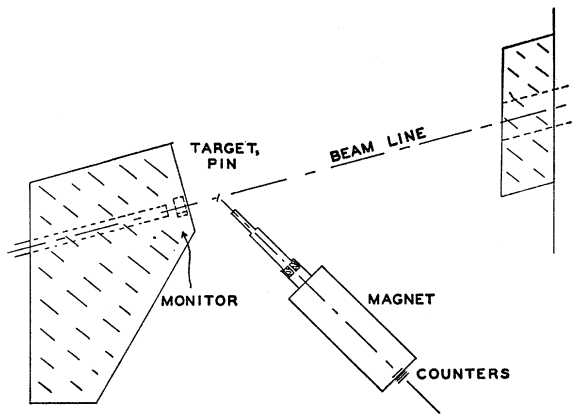

FIG. 1. Plan view of the experimental setup. Shaded areas represent shielding.

It appears that the production of low-energy pions by protons on nuclei is well studied, while little is known about the production of high-energy pions. Measurements in the latter region would be expected to yield information about the following:

(a) The behavior of the A-spectra at energies where the main effects are due to nuclear forces and the Coulomb effects are negligible.

(b) The distribution of protons and neutrons within nuclei from the comparison of the A-spectra with theory.

(c) The dependence, for light elements, of the production of high-energy pions on the momentum distribution in the nucleus.

It is the main purpose of this experiment to provide data for the production of charged pions of kinetic energy in the range 80 to 250 Mev by 450-Mev protons on Be, C, Al, Cu, Sn, Sb, Au, Pb, and U.

The experiment will also measure the energy spectrum for pion production on carbon up to the highest possible pion energies, namely those corresponding to the reaction

$$p+C^{12}\rightarrow\pi^+ + C^{13},$$

with C^{13} left unexcited. Meshcheriakov *et al.*[9] and Azhgirei *et al.*[10] have both observed tails on the pion spectrum produced by 660-Mev protons on carbon, but

[9] M. G. Meshcheriakov, I. K. Vzorov, V. P. Zrelov, B. S. Neganov, and A. F. Shabudin, Proceedings of the CERN Symposium on High-Energy Accelerators and Pion Physics, Geneva, 1956 (European Organization of Nuclear Research, Geneva, 1956), Vol. 2, p. 357.

[10] L. S. Azhgirei, I. K. Vzorov, V. P. Zrelov, M. G. Mescheriakov, and V. I. Petrukhin, Soviet Phys.—JETP **6**, 939 (1958).

their measurements were stopped about 60 Mev below the maximum energy.

II. THE EXPERIMENT

A. Experimental Procedure

The experimental procedure was, in general, as follows:

Pions, produced by the 450-Mev protons of the external beam of the Chicago synchrocyclotron in collision with the target nuclei, were detected by a fourfold scintillation counter telescope. The proton beam was monitored by a secondary emission monitor.[11]

The definition of a pion was made by simultaneous momentum and energy determination. The momentum of the particles recorded was determined by a spectrometer magnet which focused the desired particles on the counter telescope. The energy of the particles was given by the pulse height produced by the particle in one of the counters, as recorded on a pulse-height analyzer. Care was taken to make the pulses from this counter proportional to the energy loss of the particles in the scintillator. The pulses from the pions of the selected momentum then fell into channels specified by the energy loss and were counted. There was, however, in most cases very little difference between the channels assigned to pions and muons of the same momentum. How these particles were separated is dealt with in the section on the reduction of data.

The number of pions counted per unit monitored beam was directly proportional to the production cross section. The absolute cross sections were determined by a comparison with proton-proton elastic scattering measured by the use of carbon and polyethylene targets in the same setup.

The production cross sections were thus measured for the elements Be, C, Al, Cu, Sn, Sb, Au, Pb, and U. The cross sections for positive pions were obtained at a laboratory angle of 21.5° at the energies 83, 132, 166, 200, and 236 Mev and at an energy of 149 Mev at 60°. For negative pions the energies were 132, 166, and 200 Mev at 21.5° and 99 Mev at 60°. The energy intervals accepted were of the order of 1% of the energy of the pions.

For carbon the energy spectrum of the cross section was measured in the range of 44 to 335 Mev for pions of both charges at 21.5° and 60°.

B. General Layout, Beam

The 450-Mev Chicago synchrocyclotron external proton beam, focused by two strong-focusing magnets, was made to strike a target about 25 m from the cyclotron (Fig. 1). Except for a length of 50 cm at the focus of the first magnet, the beam traveled this distance in vacuum. At the target the shape of the beam was roughly circular with a diameter of about 1 cm. The beam was monitored by a secondary emission monitor[11] which, according to earlier calibrations,[12] was stable to about 1%.

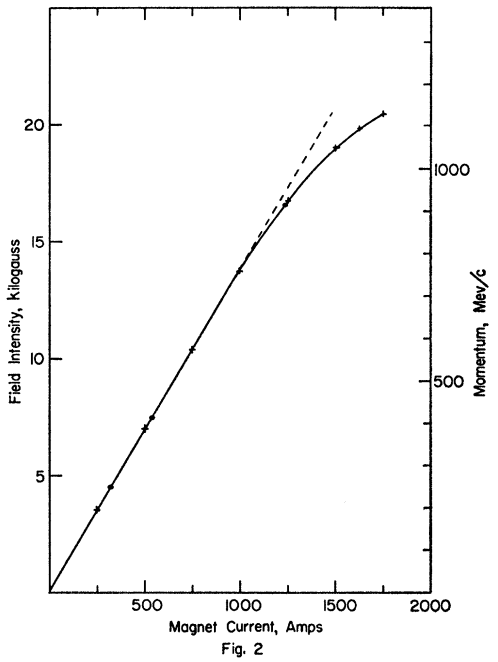

FIG. 2. Magnet excitation curve. The crosses represent field measurements with a magnetoresistance probe. The filled circles show current-momentum normalization points obtained from proton-proton elastic scattering and the reaction $p+p \rightarrow \pi^{+}+d$.

The targets were squares of side 5 cm with thickness corresponding to about 1.5 g cm^{-2} of material. They were mounted on a remotely controlled target changer centered on a pin which also served as a center of rotation for the spectrometer magnet.

After leaving the target, the scattered particles again traveled in vacuum through the spectrometer magnet until reaching the counter telescope.

C. Spectrometer Magnet

The magnet[13] is a 60° vertically deflecting wedge magnet which brought the particles to a radial focus, but defocused them in the direction perpendicular to the particle path and the radius of curvature of the path, producing an image about 10 cm long. Its aperture, in the shape of a 2.5 cm×6.35 cm rectangle, defined a solid angle of 2.5×10^{-4} steradian with an azimuthal angle of acceptance of 0.75°. The magnet could be set to analyze the particles at any angle between 8° and 150° with an accuracy of 0.1° in the region used during the experiment.

The magnetic field was measured before the experiment, using a magneto-resistance probe constructed by

[11] H. R. Fechter and G. W. Tautfest, Rev. Sci. Instr. **26**, 229 (1955).

[12] L. G. Pondrom, Phys. Rev. **114**, 1623 (1959).

[13] A. V. Crewe, Rev. Sci. Instr. **29**, 880 (1958).

Charles Rey of this Institute. Since the momentum of the analyzed particles was defined by the magnet only, it was of great interest to study the hysteresis effects. It was found that if the field was always set by decreasing the current in the coils, the reproducibility was better than ± 2 gauss in the region of interest. Fields reached by increasing the magnitude of the current were constant only to about ± 7 gauss and could differ from those obtained by decreasing the current by as much as 20 gauss. During the experiment the fields were, therefore, always obtained by first exciting the magnet to a high field intensity. The magnet current was regulated by a magnet controller that kept the current stable to one part in 20 000. Figure 2 shows the magnetic field and the corresponding momentum of the analyzed particles as function of the current.

The momentum corresponding to a given current was determined by studying proton-proton elastic scattering and the reaction $p+p \rightarrow \pi^+ + d$. Figure 3 shows a peak obtained for elastically scattered protons at 21.5°. The magnet current at the center of the peak corresponded to the momentum deduced from kinematic considerations. The centers of the peaks were determined by fitting parabolas to the upper parts and then locating their maxima.

The results of the two methods of determining the excitation curve of the magnet are in excellent agreement as can be seen from Fig. 2, where the field measurements are plotted as crosses and the momentum measurements as filled circles.

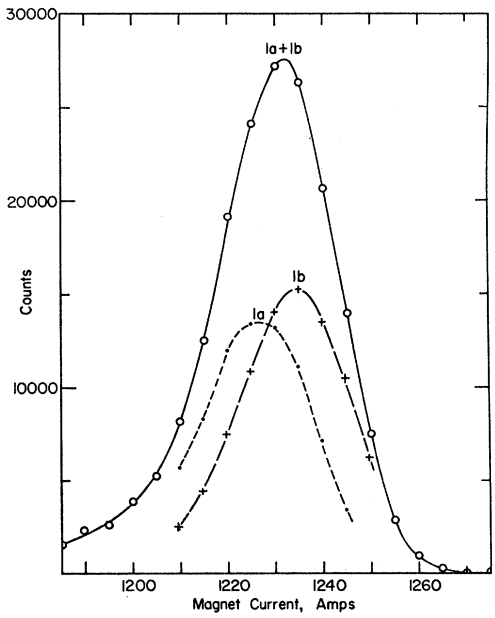

FIG. 3. A peak resulting from proton-proton elastic scattering. The high curve ($1a+1b$) is used for calibration of the solid angle of acceptance of the spectrometer magnet. Its center gives a current-momentum normalization point. The curves $1a$ and $1b$ are used to determine the momentum range (Δp) accepted by the counter telescope.

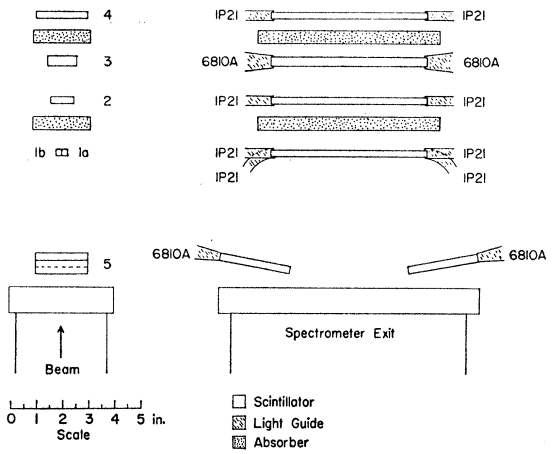

FIG. 4. Counter telescope. The beam enters from below.

D. Counter Telescope and Electronics

The counter telescope with its dimensions is sketched in Fig. 4. Counter 1, split into two parallel scintillators, $1a$ and $1b$, served as the defining counter. The three other scintillators were made sufficiently wide to accept the total beam defined by counter 1, including the spread due to the divergence of the beam (about 5°) and the multiple scattering. The two scintillators $5a$ and $5b$ were used in anticoincidence with the telescope to reduce the solid angle for acceptance of cosmic rays and general room background. Space was also provided for absorbers to stop the protons scattered from the target.

Figure 5 shows a block diagram of the essential parts of the electronics system. In general, the pulses were amplified and passed through suitable delays to a 10-nanosecond (nsec) coincidence circuit. The pulses from counters 1 and 3, however, were split in order to serve a more special purpose.

One of the pulses from counter 1 was delayed by 56 nsec more than the other. The extra delay corresponds to the time difference between two rf bunches of protons from the cyclotron, the frequency of the rotating protons in the cyclotron being about 18 Mc/sec at the time of ejection. By requiring coincidences between these delayed pulses and the pulses from the other four counters, the counting rate due to accidental coincidences was obtained under circumstances identical to those under which the pions were counted.

The signal from the third scintillator was split with one part going into the coincidence circuit while the other part was analyzed on a transistorized 400-channel pulse-height analyzer. The 30-nsec gate used in connection with the pulse-height analysis was constructed by Gabriel.[14] It was completely transistorized and could accept signal pulses up to 8 volts, with some nonlinearity as the pulse height approached this upper limit. The gate was opened by a 1-volt negative pulse given by a 12345 coincidence.

[14] R. Gabriel (private communication).

III. REDUCTION OF DATA

A. Background

A representative pulse-height spectrum T, as obtained with a target positioned in the beam, is shown in Fig. 6 together with a spectrum E, taken with an empty target holder in the beam. It is clear from these spectra that there are background counts which are due to the target and which cannot be eliminated by merely taking the difference between T and E. An analysis of the possible sources of background counts is, therefore, necessary. These sources are as follows:

(1) Some particles coming from the general room background proceed through all the counters producing apparently real events.

(2) Pions decay on their way to the telescope producing high-energy muons. In most cases, if these muons go through the telescope they cannot be separated from the pions by pulse height, since both particles are minimum ionizing.

(3) Neutral pions produced in the target decay into gamma rays which, in turn, produce electron pairs. These electrons may penetrate all counters and be registered.

(4) Due to the high counting rates in the single counters, one may expect accidental coincidences.

The background due to points (3) and (4) above can be neglected on the following grounds: In order to penetrate the telescope, an electron needed a kinetic energy $\gtrsim 10$ Mev. Such a highly relativistic electron had in counter 3 an energy loss greater than that of a minimum ionizing particle, producing pulse heights corresponding to channels 34 to 50. To check if the electrons were present, the magnet was set to analyze negative particles. A spectrum was taken with a carbon target and a matched CH_2 target. From the CH_2 target could come only positive and neutral pions in excess of the pions from the carbon target. In the electron channels an excess of 6 ± 12 counts were registered, while there were 312 counts in the pion channels (16 to 36) with an excess of 43 ± 25 with the CH_2 target in. In addition to being small, the electron background was in most cases separated from the pions by the pulse-height analysis. The accidental coincidences were registered as explained in the discussion of the electronics. This counting rate corresponded to not more than 3 per thousand counts registered and could, therefore, be neglected.

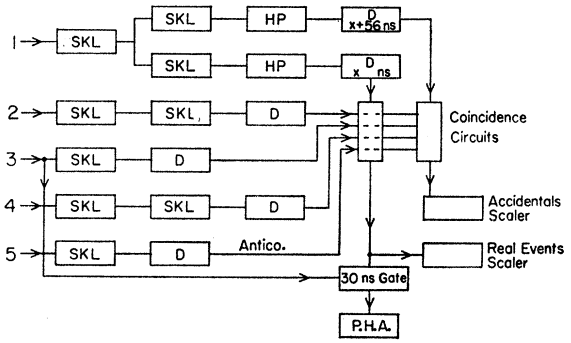

FIG. 5. Block diagram showing the essential parts of the electronics system. SKL = Spencer-Kennedy wide-band amplifier, HP = Hewlett-Packard wide-band amplifier, D = Delay line, PHA = Pulse-height analyzer.

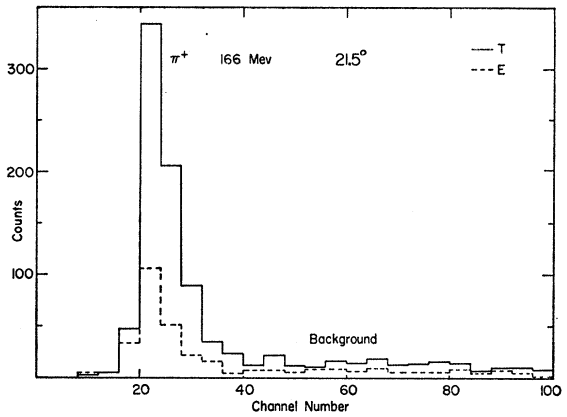

FIG. 6. Representative pulse-height spectrum taken with target in the beam, T, and with an empty target holder in the beam, E. The magnetic field corresponded to $p = 272$ Mev/c ($T_\pi = 166$ Mev).

The general room background consisted of one part due to scattering of the beam in air, pipewalls, etc. This was target independent and was subtracted out when the difference was taken between a T spectrum and an E spectrum. Another part was target dependent and could be treated together with the background in point 2 above.

There were two main contributors to the target dependent background, namely pions and protons. As seen from Figs. 7(a) and (b), the background due to the two kinds of particles could be detected by studying the case of low-energy pions (44 Mev) at two angles. In this case, the desired pions appeared in a peak well separated from a peak due to the background of high-energy pions and muons. The difference, $T-E$, for this background was reduced by a factor of about 2 in going from 21.5° to 60°, while the events in channels higher than those of the pions were reduced by a factor of 12 for the same angular change. The first factor compares favorably with the reduction in the cross section for pion production, while the latter factor is consistent with the great reduction in elastically and inelastically scattered protons as the angle is increased.[15]

Finally, it became apparent from a study of spectra for pion energies greater than 300 Mev that proton-induced background was important only for channels higher than 36, so that it could be neglected in most cases. The pion-induced background in the low channels remained also beyond 300 Mev. It had to be estimated

[15] R. E. Richardson, W. P. Ball, C. E. Leith, Jr., and B. J. Moyer, Phys. Rev. 86, 29 (1952); H. Tyren and Th. A. J. Maris, Nuclear Phys. 3, 52 (1957).

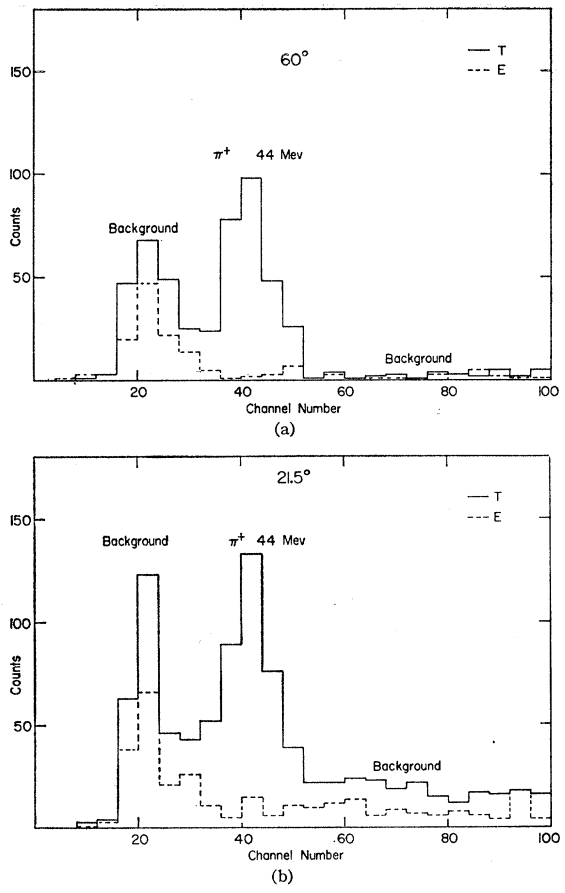

FIG. 7. Pulse-height spectra for 44-Mev positive pions. 7(a) and 7(b) represent the laboratory angles 21.5° and 60°, respectively.

for each pion energy studied, but since these events were produced in proportion to the pion production, they did not affect the ratios between cross sections taken for different targets at a fixed pion energy.

B. Relative Cross Sections

The main purpose of this experiment is to find the relative cross sections for pion production as a function of atomic mass number. The number of pions was obtained by taking the difference between the counts in the proper channels of the pulse-height spectra obtained with target in position and with the target out. The target-dependent background had no effect on the A-spectra, except for a slight amount of proton-induced events in the case of 83-Mev pions. Background due to pions did not have to be subtracted out since it was proportional to the effect.

The number of counts obtained in this way was divided by the number of atoms per square centimeter for each target giving a number directly proportional to the cross section.

The target thickness was measured to an accuracy better than 1%, except for Sb where the error could be as large as ±3%.

C. Absolute Cross Sections

In order to discuss the method of deducing the absolute cross section, it is useful to consider the formula for obtaining the number of counts Δ^2N, for the bombardment of a target with N_t nuclei per cm^2 by N_b protons:

$$\Delta^2N = N_bN_tDA(d^2\sigma/d\Omega dE)\Delta\Omega\Delta E.$$

Here, $\Delta\Omega$ is the solid angle of acceptance of the magnet, ΔE represents the energy interval accepted, D is a factor representing the decay of the pions, and A represents the absorption of the pions in scintillators and absorbers. These quantities are obtained in the following way.

ΔE may be rewritten as $(pc/E)\Delta p=\beta\Delta p$. Δp is measured by the use of counters 1a and 1b. As one scans across a peak (e.g., elastically scattered protons) with the magnet the peaks registered by counters 1a and 1b are shifted due to their physical separation (see Figs. 3 and 4). The separation of the peak centers converted into momentum units is equivalent to the center-center separation of the scintillators 1a and 1b. Finally, the Δp measured in this way is multiplied by the ratio of the total width of 1a plus 1b to their center-center distance. The separation between the two peaks was found by fitting parabolas to the tops and finding their centers, while the scintillator separation was measured with a traveling microscope. The inaccuracies in these determinations are of the order of 4%. $\Delta p/p$ was found to be a monotonically increasing function of p with values ranging from 0.6% to 1.3% in the region of interest. This is in good agreement with earlier values.[16]

$N_b\Delta\Omega$ is determined as one quantity by normalizing the number of counts obtained in a peak of protons elastically scattered by protons to published data.[17] The statistical accuracy is better than 1%, while the published data are accurate to about 3%.

D, the decay factor, was calculated by taking the half-life of the pions to be 2.56×10^{-8} nsec.

The absorption of the pions in scintillators and absorbers is estimated in the following way: Geometrical cross sections are assumed for the atoms of aluminum and copper absorbers and also for the carbon atoms in the scintillators, while the cross section of the hydrogen in the scintillators was varied with energy in accordance with published data on the scattering of charged pions on protons. The absorption factor A was generally of the order of 1.15.

Due to the uncertainties in the determination of these factors, the absolute cross sections have systematic probable errors of about 8% in addition to those errors that enter into the relative cross sections. The systematic errors are not included in Tables and Diagrams.

[16] A. V. Crewe, B. Ledley, E. Lillethun, S. Marcowitz, and L. G. Pondrom, Phys. Rev. **114**, 1361 (1959).
[17] W. N. Hess, Revs. Modern Phys. **30**, 368 (1958).

TABLE II. Differential cross sections for the production of charged pions by 450-Mev protons on various nuclei. Cross sections are given in units of μb(sr Mev)$^{-1}$.

T_π (Mev)	Be	C	Al	Cu	Sn	Sb	Au	Pb	U
				π^+, $\theta_{lab}=21.5°$					
83	42.3 ±1.1	55.1 ±1.5	81.8 ±2.6	102.1±5.1	110.7±5.5		126.5± 8.4	119.1±10.3	138.4±10.4
132	58.9 ±1.3	70.4 ±1.1	98.6 ±2.3	130.8±4.8	124.1±4.9	116.6±7.9	136.5±10.8	137.9± 9.2	149.5± 8.9
166	51.7 ±0.75	64.1 ±0.8	82.4 ±1.3	104.1±1.8	112.5±2.7	105.0±3.0	113.7± 4.0	115.1± 4.9	117.2± 4.0
200	33.2 ±0.7	43.9 ±0.8	55.4 ±1.0	70.7±2.0	71.5±2.5	66.9±2.6	70.7± 3.7	72.0± 4.6	78.3± 4.6
236	12.7 ±0.3	17.0 ±0.4	24.1 ±0.4	30.3±0.9	28.5±0.9	24.9±1.5	25.9± 1.9	30.5± 2.3	31.3± 2.3
				π^+, $\theta_{lab}=60°$					
149	8.0 ±0.3	11.4 ±0.4	16.3 ±0.6	21.2±1.0	23.0±1.5	27.6±2.0	30.2± 2.6	29.4± 3.2	27.7± 2.4
				π^-, $\theta_{lab}=21.5°$					
132	5.61±0.44	5.55±0.37	7.9 ±0.8	13.3±1.3	17.8±2.6	15.3±2.4	18.5± 2.8	21.0± 3.6	26.5± 3.6
166	4.53±0.22	4.13±0.28	6.53±0.47	9.2±0.7	11.9±0.9	13.8±1.1	15.2± 2.2		18.6± 2.2
200	2.27±0.23	1.73±0.31	3.8 +0.5	4.1±0.8	3.9±1.1	3.4±2.0	7.6± 2.0	3.5± 2.5	5.4± 2.0
				π^-, $\theta_{lab}=60°$					
99		2.2 ±0.5		4.4±1.3			10.1± 3.3	12.4± 5.0	10.8± 4.1

The target-dependent background has been clearly separated from the events of interest only in measurements at the extremes of the energy spectra for carbon. By fitting smooth curves through these points, the background was estimated for other elements and energies. This, however, introduces a rather large error depending on the target and pion energy in question. [These uncertainties are included in the values given in Tables II–IV and in the diagrams of the carbon spectra (Figs. 12 and 13), while they have been left out of the diagrams showing A-spectra (Figs. 9–11).]

IV. THEORETICAL MODEL

The model used in the calculation of the A-spectra is in general agreement with the models used by Gasiorowicz,[8] Merritt and Hamlin,[4] and Ansel'm and Shekhter.[18] The model is discussed in detail in the Appendix.

The determining effects are assumed to be due to (i) the absorption of the incoming proton and the outgoing pion within the nucleus, and (ii) a surface layer of neutrons on the nuclei.

The nucleus is taken to consist of a core of radius R_p in which there are equal numbers of protons and neutrons, amounting to $2Z$ nucleons, and a surface layer of the same density due to the $A-2Z$ excess neutrons, reaching out to a radius R_n. R_n has been chosen to be

$$R_n=1.35\times A^{\frac{1}{3}}\times 10^{-13}\text{ cm},$$

in agreement with the potential radius given by Seth.[19] This value was obtained from low-energy neutron scattering experiments. The radius of the core then becomes $R_p=1.35\times(2Z)^{\frac{1}{3}}\times 10^{-13}$ cm.

The A-spectra are proportional to the integral

$$\sigma \propto \int\int\int_{\text{sphere}} \exp[-(s_{11}\eta_{11}+s_{12}\eta_{12})-(s_{21}\eta_{21}+s_{22}\eta_{22})]dv,$$

where η_{11} and η_{12} are the absorption coefficients for protons in the surface layer and the core, respectively, and η_{22} and η_{21} are the absorption coefficients for the pions for the same regions. The S_{ij} are defined in Fig. 8 which is a cut through the center of the nucleus in the plane of scattering, showing a production of a pion at P. The integration over a sphere was performed by an IBM-709 computer.

The proton absorption coefficients were computed from the total pp and pn cross sections. Since these are almost the same at the energies in question, η_{11} was set equal to η_{12}. Their value is 0.182×10^{13} cm^{-1}.

The pion absorption coefficients were obtained from the values quoted by Frank *et al.*[20] and are listed in Table V.

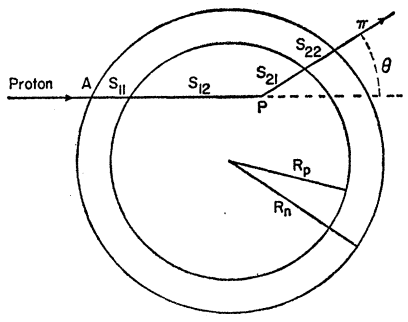

FIG. 8. Model of nucleus. The outer shell is assumed to contain neutrons only. Proton enters the nucleus at A, creates a pion at P. The pion leaves the nucleus at a laboratory angle $\theta°$ with respect to incoming protons. Protons and pions are attenuated as they proceed through the nucleus, following the paths S_{ij}.

[18] A. A. Ansel'm and V. M. Shekhter, Soviet Phys.—JETP **6**, 376 (1958).
[19] K. K. Seth, Revs. Modern Phys. **30**, 442 (1958).
[20] R. M. Frank, J. L. Gammel, and K. M. Watson, Phys. Rev. **101**, 891 (1956).

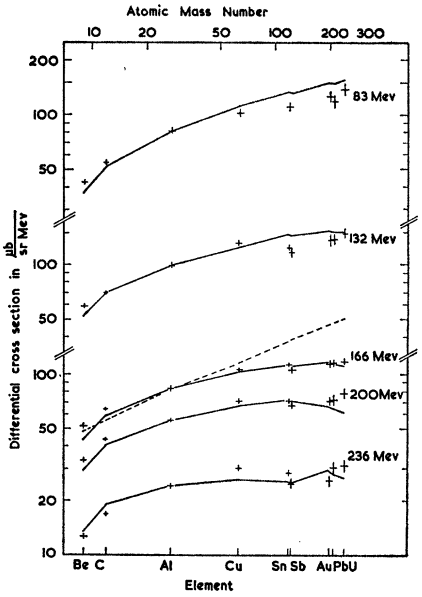

FIG. 9. A-spectra for positive pions produced at a laboratory angle of 21.5°. The energies quoted refer to the laboratory energies of the pions. Note the discontinuities in the ordinate. The curves are theoretical, the full ones based on a model with a neutron shell on the outside of the nucleus, the broken one assuming equal distribution of protons and neutrons. The curves are normalized to aluminum.

V. RESULTS AND CONCLUSIONS

A. A-Spectra

The properties of the A-spectra of Figs. 9 to 11 can be summarized as follows:

1. The spectra for negative pions are always much steeper than those for the positive pions of the same energy. The ratio of π^+ to π^- yield depends on the element, and for all energies goes through a maximum for carbon in agreement with the findings of Meshkovskii *et al.*[6] This favors the idea of having a neutron shell on the outside of the nucleus, as explained in the Introduction.

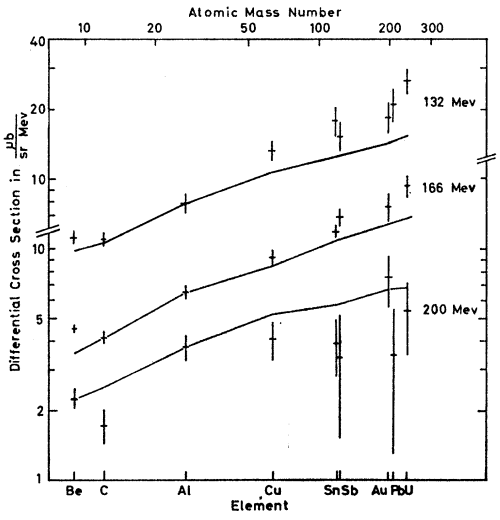

FIG. 10. A-spectra for negative pions produced at 21.5°. The energies quoted refer to the laboratory energies of the pions. The curves are theoretical, normalized to aluminum.

TABLE III. Relative yield.

Pion energy (Mev)	Be yield/U yield	Al yield/U yield
83	0.305±0.025	0.59±0.05
132	0.395±0.025	0.66±0.04
166	0.441±0.016	0.70±0.03
200	0.424±0.026	0.71±0.04
236	0.406±0.031	0.77±0.06

2. The cross section for production of positive pions of given energy on carbon is always considerably greater than that for beryllium, while the cross sections for negative pions at the same energies are nearly the same for the two elements. This again speaks in favor of a neutron shell, and agrees with the results of Meshkovskii *et al.*,[6] and of experiments on the reaction $Li^7(Be^9Be^8)Li^8$,[21] in Allison's[22] interpretation. He has shown that in order to explain the results from the latter experiments one must assume the neutrons in beryllium to be spread out over a considerable volume, with a density decreasing essentially exponentially with R, still being non-negligible at perinuclear distances of the order of 10^{-12} cm.

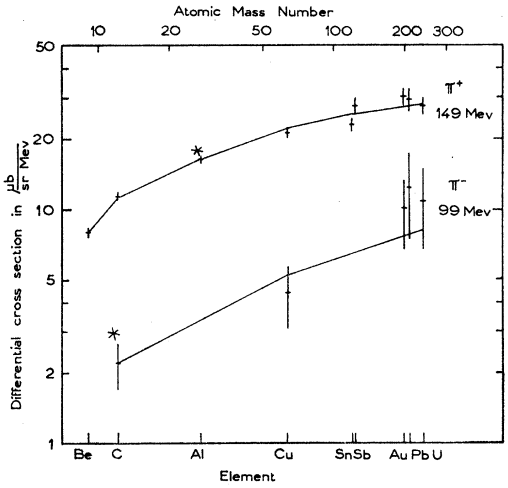

FIG. 11. A-spectra for positive and negative pions produced at 60° with laboratory energies as indicated. The curves are theoretical, normalized to the points marked with an asterisk.

3. The spectra are energy dependent in contradiction to the assumption made by Meshkovskii *et al.*[6] This is shown by the values in Table III where the yields from beryllium and aluminum have been divided by the uranium yield.

[21] E. Norbeck, Jr. and C. S. Littlejohn, Phys. Rev. **108**, 754 (1957). E. Norbeck, Jr., J. M. Blair, L. Pinsonneault, and R. J. Gerbracht, *ibid.* **116**, 1560 (1959).

[22] S. K. Allison, Phys. Rev. **119**, 1975 (1960).

It is seen that the aluminum to uranium ratio increases monotonically with energy, while the beryllium to uranium ratio goes through a maximum for $T_\pi = 166$ Mev. The latter is probably due to the internal momentum distribution in the nuclei, with nucleons of lower momentum in the light nuclei.

4. The targets of $_{50}$Sn and $_{51}$Sb had been chosen in order to see if there were any effects due to the magic number of protons in Sn. Indeed, for positive pions the cross section for Sn is constantly about 7% higher than the cross section for Sb at 21.5°. In order to decide whether the difference is significant or not, the experiment would have to be repeated with greater accuracy.

The curves in the Figs. 9 to 11 show the A-spectra computed according to the theory described in the Appendix. The spectra are normalized to the aluminum point, except in the case of 99-Mev negative pions at 60° where carbon is the normalization point. There is a general agreement between the experimental and theoretical data as far as the energy and charge dependence of the A-spectra is concerned. The following points should be noted.

The theoretical curves for positive pions at 21.5° (Fig. 9) show a greater energy dependence than found experimentally, and those of the negative pions of $T_\pi = 132$ Mev and 166 Mev at the same angle (Fig. 10) both fall below the experimental data for elements of high atomic mass number. This is partly due to the simplified calculation, assuming positive pions to be produced on protons only, and negative pions to be produced with equal frequency on protons and neutrons. However, this discrepancy also suggests that the energy dependence of the pion absorption factor η_{21} as computed is not correct. The theoretical η_{21} goes through a broad maximum in the region where $T_{\pi\text{lab}}$ is $\sim$230 Mev. If this minimum is shifted toward lower energy, both the π^+ and π^- spectra would give a better general agreement with the experimental data.

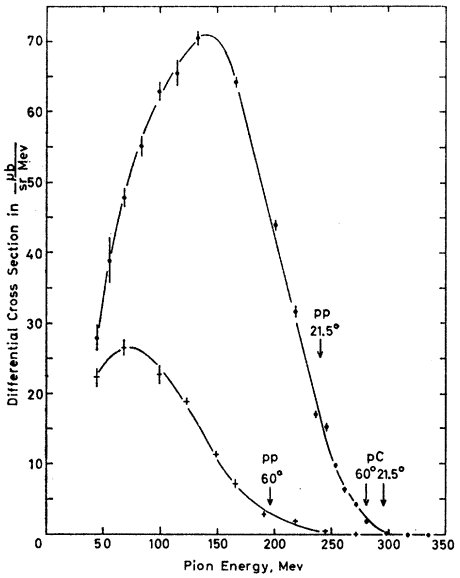

FIG. 12. Energy spectra for positive pions produced by 450-Mev protons on carbon. The laboratory scattering angle is indicated on the graph. The curves are drawn to guide the eye.

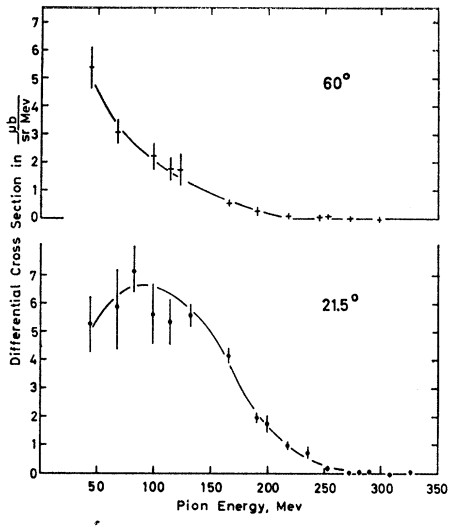

FIG. 13. Energy spectra for negative pions produced by 450-Mev protons on carbon. The laboratory scattering angle is indicated on the graph. The curves are drawn to guide the eye.

The data from the article by Frank *et al.*[20] have been used before, e.g., by Williams *et al.*[23] in their description of the Z dependence of positive photopion production. The variation of pion mean-free path in the nucleus with pion energy was also in that case found to differ from the calculated one in the same way as in this experiment.

The A-spectrum for pions of 166-Mev kinetic energy was calculated for two models, namely with (a) a neutron shell around the nucleus and (b) an equal distribution of protons and neutrons. The experimental data clearly favor the model with the neutron shell.

B. Energy Spectra

The energy spectra for carbon are shown in Figs. 12 and 13, and the cross sections are listed in Table IV.

It has been shown[24] that about 70% of the positive pions produced in proton-proton collisions at energies around 300–400 Mev come from the reaction

$$p+p \rightarrow \pi^+ + d,$$

and the spectrum shape is consistent with this. Taking into account a 25-Mev kinetic energy of the struck nucleon to account for the Fermi motion in the nucleus, the pion may obtain a maximum energy which is indicated in Fig. 12 by an arrow labeled pp. Another arrow, labeled pC, indicates the pion energy available from

[23] W. S. C. Williams, K. M. Crowe, and R. M. Friedman, Phys. Rev. **105**, 1840 (1957).

[24] M. Gell-Mann and K. Watson, Ann. Rev. Nuclear Sci. **4**, 219 (1954).

the reaction

$$p+C^{12} \rightarrow \pi^{+}+C^{13},$$

with the C^{13} nucleus left unexcited.

At 21.5° the spectrum for positive pions shows relatively high cross sections in the neighborhood of the "pC" energy (295 Mev). For negative pions, however, there is no analogous two-body reaction; and consequently the spectral shape is different in the two cases. The peak is shifted to a lower energy because of the lower average pion energy in the three-body final state, and in addition the peak is considerably broader.

The spectrum drops to zero at about 270 Mev and no negative pions were observed in the neighborhood of the "pC" energy. The only two-body reaction available would be

$$p+C^{12} \rightarrow \pi^{-}+O^{13},$$

a reaction which may be expected to occur with considerably less frequency than the corresponding one for positive pions.

At 60° both the positive and the negative spectrum decrease faster with energy, becoming negligible before reaching the "pC" energy. This suggests that it is very improbable that the nucleus may absorb the amount of momentum necessary for the production of pions of these energies, without breaking up.

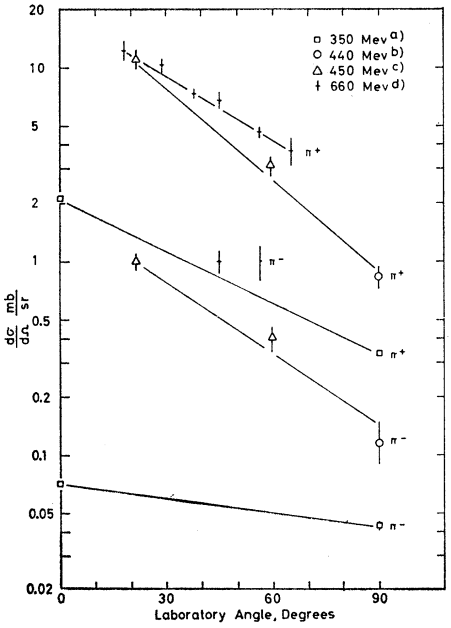

FIG. 14. Differential cross section for production of pions by protons on carbon. [a] W. F. Dudziak, University of California Radiation Laboratory Internal Report UCRL-2564, 1954 (unpublished); [b] reference 25; [c] present experiment; [d] A. G. Meshkovskii, Ia. Ia. Shalamov, and V. A. Shebanov, Soviet Phys.—JETP **7**, 987 (1958); A. G. Meshkovskii, Iu. S. Pligin, Ia. Ia. Shalamov, and V. A. Shebanov, *ibid.* **5**, 1085 (1957); reference 9.

TABLE IV. Differential cross sections for the production of charged pions by 450-Mev protons on carbon. Cross sections are given in units of μb (sr Mev)$^{-1}$.

T_π (Mev)	$\theta_{lab}=21.5°$ π^+	$\theta_{lab}=21.5°$ π^-	$\theta_{lab}=60°$ π^+	$\theta_{lab}=60°$ π^-
44	27.9 ±1.9	5.3 ±1.0	22.3 ±1.4	5.4 ±0.8
55	38.8 ±3.3			
68	47.8 ±1.4	5.9 ±1.3	26.5 ±1.1	3.1 ±0.4
83	55.1 ±1.5	7.2 ±1.0		
99	62.8 ±1.3	5.6 ±1.1	22.7 ±1.3	2.2 ±0.5
114	65.4 ±1.8	5.3 ±0.8		1.7 ±0.4
123			18.9 ±0.54	1.7 ±0.5
132	70.4 ±1.1	5.55±0.37		
149			11.36±0.44	
166	64.1 ±0.8	4.13±0.28	7.17±0.66	0.53±0.12
191		1.96±0.21	2.85±0.24	0.25±0.15
200	43.9 ±0.8	1.73±0.31		
218	31.6 ±0.9	0.98±0.16	1.93±0.34	0.07±0.09
236	17.0 ±0.4	0.72±0.23		
245	15.2 ±0.6		0.37±0.07	0.03±0.07
253	9.77±0.36	0.19±0.07		0.06±0.06
262	6.44±0.40			
272	4.24±0.23	0.02±0.07	0.16±0.12	−0.01±0.03
281	1.85±0.21	0.04±0.09		
290		0.05±0.06		
298	0.16±0.07		0.00±0.05	−0.05±0.05
308		−0.05±0.05		
317	0.00±0.06			
326		0.04±0.05		
335	0.00±0.06			

The energy spectra have been integrated to give the total differential cross section. Together with the values given by Rosenfeld[25] for production of pions on carbon by 440-Mev protons at 90°, the cross sections are listed below in units of millibarns per steradian:

	21.5°	60°	90°
π^+	11.0 ±1.0	3.1 ±0.3	0.83 ±0.11
π^-	0.95±0.11	0.43±0.06	0.115±0.024

A comparison of these data with those obtained for 350- and 660-Mev protons is shown in Fig. 14. It should be noted that the cross sections from the present experiment are almost as high as those for the case of 660-Mev protons.

ACKNOWLEDGMENTS

I am very thankful to Professor Albert V. Crewe for encouragement and helpful discussions in connection with this experiment. Thanks are also due to E. Heiberg, P. Isacsson, R. H. March, and S. M. Marcowitz for their help during the cyclotron runs and to the cyclotron crew for providing a steady proton beam. Finally, I would like to thank D. Russell for programming the theoretical calculations described in the Appendix, for the IBM-704 computer at Argonne National Laboratory, and P. Marcer for performing the computations on the IBM-709 at CERN.

[25] A. H. Rosenfeld, Phys. Rev. **96**, 130 (1954).

TABLE V. Pion absorption coefficients used in the calculation of the A-spectra. The units are 10^{13} cm^{-1}.

Element \ Pion energy (Mev)	π^+ 83	132	149	166	200	236	π^- 99	132	166	200
Be	0.417	0.666	0.715	0.770	0.910	1.00	0.526	0.715	0.834	0.910
C	0.400	0.666	0.715	0.770	0.910	1.00	0.526	0.770	0.834	0.910
Al	0.385	0.666	0.715	0.770	0.910	1.00	0.555	0.770	0.834	0.910
Cu	0.385	0.666	0.715	0.770	0.910	1.00	0.555	0.770	0.834	0.910
Sn	0.357	0.588	0.666	0.715	0.834	1.00	0.588	0.834	0.834	1.00
Sb	0.357	0.588	0.666	0.715	0.834	1.00	0.588	0.834	0.834	1.00
Au	0.333	0.555	0.625	0.666	0.834	0.910	0.666	0.834	0.834	1.00
Pb	0.333	0.555	0.625	0.666	0.834	0.910	0.666	0.834	0.834	1.00
U	0.322	0.555	0.625	0.666	0.834	0.910	0.666	0.834	0.910	1.00

APPENDIX

In considering the production of pions on nuclei, one may assume that the main process is by individual proton-nucleon collisions. There are, however, several effects which complicate the situation, such as:

(1) the velocity distribution of the nucleons in the nucleus;

(2) the Coulomb barrier;

(3) the inhibition due to the Pauli exclusion principle of the production of pions which lead to recoiling nucleons in already occupied states;

(4) the absorption of the incoming proton by processes not leading to the creation of a pion;

(5) the absorption of the pion on its way out of the nucleus, either by re-absorption in the nucleus or by scattering which results in changed energy and direction for the pion;

(6) the production of pions in collisions of the incoming proton with correlated nucleons within the nucleus (e.g., deuteron or α-particle configurations).

In the calculations leading to the predicted A-spectra, points (1), (2), (3), and (6) have been ignored. For the high-energy pions, it seems reasonable to neglect the effects of the Coulomb barrier and the Pauli exclusion principle. It may, however, seem worse to neglect the effects of the momentum distribution, since the production of high-energy pions depends largely on the presence of nucleons of relatively high momenta within the nucleus. The dependence on this distribution has indeed been shown to be quite important for light nuclei.[5] It may be assumed to be of lesser importance in the case of the heavy elements which make up the majority of the cases studied in this experiment. The same general argument may also be used about leaving out the effect of correlated nucleons.

The resulting model for the calculations, therefore, puts the emphasis on the attenuation of the protons and the pions within the nucleus. This is in general agreement with the models used by Gasiorowicz,[8] Merritt and Hamlin,[4] and Ansel'm and Shekhter.[18]

The nuclear radii are chosen according to the formula $R_n=1.35\times A^{\frac{1}{3}}\times 10^{-13}$ cm. This radius, which agrees with the potential radius given by Seth,[19] is in the present calculation taken to define the distance to which the neutrons are distributed. The protons are assumed to extend only to a radius of $R_p=1.35\times(2Z)^{\frac{1}{3}}\times 10^{-13}$ cm. The resulting model is a sphere of uniform mass density, but with the neutrons in excess of the number of protons placed in a surface shell.

On the basis of isotopic spin considerations, taking into account that the pions are produced mainly when a nucleon is excited to a $\frac{3}{2}$ state in the isotopic spin space, the ratio of positive pions produced in the core, to those produced in the shell should be as 11:2 per volume element. For negative pions this ratio should be 1:2.[26] However, for the sake of simplicity in the calculation, the positive pions have been assumed to be produced in proton-proton collisions only and the negative pions with equal probability in both proton-proton and proton-neutron collisions. The main effect of this simplification will be to reduce the yields of positive pions from the heavy elements where the neutron shell is relatively thick.

Figure 8 shows a cut through the nucleus in the plane of scattering. An A-spectrum will be proportional to the value defined by the integral

$$\sigma \propto \int\int\int_{\text{sphere}} \exp[-(s_{11}\eta_{11}+s_{12}\eta_{12})-(s_{21}\eta_{21}+s_{22}\eta_{22})]dv.$$

Here, η_{11} represents the proton absorption coefficient in pure neutron matter, while η_{12} represents the same quantity in an equal mixture of neutrons and protons. Similarly, η_{21} and η_{22} are the absorption coefficients for pions in an equal mixture and in pure neutron matter, respectively. The paths S_{ij} are defined by Fig. 8 where the pion is assumed to be created at P.

Since equal density was assumed throughout the nucleus, η_{11} has been set equal to η_{12}, assuming that the proton absorption is proportional to the total pp and pn scattering cross sections which are almost equal at the energies in question. The value for η_{11}, computed from an average of these cross sections, was found to be $\eta_{11}=0.182\times 10^{13}$ cm^{-1}.

[26] H. A. Bethe and F. de Hoffmann, *Mesons and Fields* (Row, Peterson and Company, Evanston, Illinois, 1955), Vol. II, p. 336.

For positive pions $\eta_{21}=2\eta_{22}$ on the basis of the total scattering cross sections in this energy range. η_{21} was taken from the values given by Frank *et al.*[20] The data are given as a function of the kinetic energy of the pion within the nucleus, measured in the laboratory frame of reference. In order to find this energy, the nuclear potential is included in the way specified by Frank *et al.*, and finally the energy was adjusted by adding or subtracting the Coulomb potential energy corresponding to a particle of unit charge at R_p for negative and positive pions, respectively. The values of η_{21} are listed in Table V.

PHYSICAL REVIEW VOLUME 125, NUMBER 2 JANUARY 15, 1962

Pion Production in Pion-Nucleon Collisions and the Pion-Pion Interaction*

EMMA PEREZ FERREIRA
Comisión Nacional de Energía Atómica, Buenos Aires, Argentina
(Received July 31, 1961)

The momentum distributions of the pions of all charge states produced in the interaction of 960-Mev π^- mesons with protons are calculated on the assumption of a primary $\pi-\pi$ interaction followed by a $\pi-N$ interaction with excitation of the (3,3) isobar state of the nucleon. The predicted spectra are in reasonable agreement with experimental data when the $\pi-\pi$ resonance energy is assumed to be about 700 Mev.

EXPERIMENTAL results[1] on single pion production in π^-+p collisions at 960 Mev were found to be in reasonable agreement with the predictions of the isobar model[2] regarding both branching ratios and momentum distributions of the final pions in the two possible reactions:

$$\pi^-+p\rightarrow\pi^-+\pi^++n, \quad \text{(I)}$$

$$\pi^-+p\rightarrow\pi^-+\pi^0+p. \quad \text{(II)}$$

However, a similar experiment[3] performed at 1 Bev showed some discrepancies with the predicted momentum distribution of the final pions of reaction II. Selleri[4] and Landovitz and Marshall[5] have recently suggested that those discrepancies could be due to the rapid onset of a different process, in addition to pion-nucleon resonances, viz. a pion-pion resonance, which, for instance, is necessary in order to account for the nucleon electromagnetic structure, as well as for the low-energy pion-nucleon phase shifts.[6] These authors proposed therefore a model, according to which the production process should start with the interaction between the incoming pion and a pion of the cloud. Then, a final-state interaction would excite the nucleon to the (3,3) isobar state, with a further decay into a pion and a nucleon.

Some attempts[4,7–10] have been made in order to justify through that predominant one-pion exchange (with or without final-state interaction), the behavior of the total pion-nucleon cross sections, in particular, the maximum in the π^-+p interaction at 900 Mev and in π^++p at 1400 Mev. Furthermore, several authors have investigated the possible influence of the pion-pion interaction in pion production through the analysis of the energy spectrum of the secondary nucleon in the laboratory frame of reference,[11,12] of charge state branching ratios[7,13] and by means of the more refined method suggested by Chew and Low[14] which was recently applied by Anderson *et al.*[15] to their experimental results. Neither the latter method nor the semi-phenomenological treatment have led to any definite

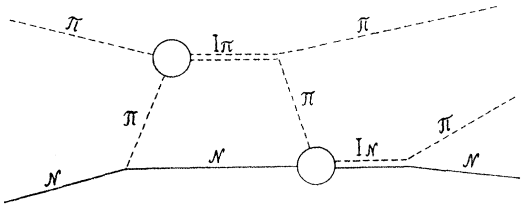

FIG. 1. Diagram for the pion production process. I_π stands for the $T=J=1$ di-pion state and I_N for the $T=J=\frac{3}{2}$ nucleon isobar.

* This is part of a work submitted to the Faculty of Sciences of the University of Buenos Aires, in partial fulfillment of the requirements for the degree of Doctor in Physics.

[1] V. Alles-Borelli, S. Bergia, E. Perez Ferreira, and P. Waloschek, Nuovo cimento **14**, 211 (1959).

[2] R. B. Sternheimer and S. J. Lindenbaum, Phys. Rev. **109**, 1723 (1958).

[3] I. Derado and N. Schmitz, Phys. Rev. **118**, 309 (1960).

[4] F. Selleri, Nuovo cimento **16**, 775 (1960).

[5] L. Landovitz and L. Marshall, Phys. Rev. Letters **4**, 474 (1960).

[6] J. Bowcock, W. N. Cottingham, and D. Lurié, Phys. Rev. Letters **5**, 386 (1960).

[7] P. Carruthers and H. A. Bethe, Phys. Rev. Letters **4**, 536 (1960).

[8] R. F. Peierls, Phys. Rev. Letters **5**, 166 (1960).

[9] F. J. Dyson, Phys. Rev. **99**, 1037 (1955).

[10] G. Takeda, Phys. Rev. **100**, 440 (1955).

[11] F. Bonsignori and F. Selleri, Nuovo cimento **15**, 465 (1960).

[12] I. Derado, Nuovo cimento **15**, 853 (1960).

[13] B. A. Muir, E. Pickup, D. K. Robinson, and E. O. Salant, Phys. Rev. Letters **6**, 192 (1961).

[14] G. F. Chew and F. E. Low, Phys. Rev. **113**, 1640 (1959).

[15] J. A. Anderson, V. X. Bang, P. G. Burke, D. D. Carmony, and N. Schmitz, Phys. Rev. Letters **6**, 365 (1961).